International Journal of Approximate Reasoning 50 (2009) 680–693

Contents lists available at ScienceDirect

International Journal of Approximate Reasoning

journal homepage: www.elsevier.com/locate/ijar

Classical and imprecise probability methods for sensitivity analysis in engineering: A case study

Michael Oberguggenberger [a,*], Julian King [b,1], Bernhard Schmelzer [a]

[a] Universität Innsbruck, Institut für Grundlagen der Bauingenieurwissenschaften, Technikerstr. 13, A-6020 Innsbruck, Austria
[b] Österreichische Akademie der Wissenschaften, Forschungsstelle für Atemgasanalytik, A-6850 Dornbirn, Austria

ARTICLE INFO

Article history:
Received 29 December 2007
Accepted 30 September 2008
Available online 11 October 2008

MSC:
04E72
60D05
62P30
65C05
65N30

Keywords:
Reliability of structures
Sensitivity analysis
Random sets
Fuzzy sets
Simulation methods
Aerospace engineering

ABSTRACT

This article addresses questions of sensitivity of output values in engineering models with respect to variations in the input parameters. Such an analysis is an important ingredient in the assessment of the safety and reliability of structures. A major challenge in engineering applications lies in the fact that high computational costs have to be faced. Methods have to be developed that admit assertions about the sensitivity of the output with as few computations as possible. This article serves to explore various techniques from precise and imprecise probability theory that may contribute to achieving this goal. It is a case study using an aerospace engineering example and compares sensitivity analysis methods based on random sets, fuzzy sets, interval spreads simulated with the aid of the Cauchy distribution, and sensitivity indices calculated by direct Monte Carlo simulation. Computational cost, accuracy, interpretability, ability to incorporate correlated input and applicability to large scale problems will be discussed.

1. Introduction

The goal of this article is to demonstrate how various methods from probability theory and imprecise probability theory can be employed in sensitivity analysis of engineering structures. We are motivated by a research project in aerospace engineering[2] which involved the determination of the buckling load of the frontskirt of the ARIANE 5 launcher under various loading and flight scenarios. The frontskirt is a reinforced light weight shell structure. The computation of the decisive parameter indicating failure, the load proportionality factor (LPF), is based on a finite element model.[3] Part of the project was to determine the most influential input parameters (loads, material constants, geometry) on the load proportionality factor in a sensitivity

* Corresponding author.
E-mail addresses: michael.oberguggenberger@uibk.ac.at (M. Oberguggenberger), jking@oeaw.ac.at (J. King), bernhard.schmelzer@uibk.ac.at (B. Schmelzer).
URLs: http://techmath.uibk.ac.at (M. Oberguggenberger), http://techmath.uibk.ac.at (B. Schmelzer).

[1] Recipient of a DOC-fellowship of the Austrian Academy of Sciences at the Breath Research Unit.

[2] ICONA-project, Intales GmbH Engineering Solutions and University of Innsbruck, supported by TransIT Innsbruck and by EADS Astrium ST.

[3] The load proportionality factor is defined as the limiting value in an incremental procedure in which the dynamic loads during a flight scenario are increased step by step until breakdown of the structure is reached.

0888-613X/$ - see front matter © 2008 Published by Elsevier Inc.
doi:10.1016/j.ijar.2008.09.004

analysis. The goal was to evaluate the design and to assess the safety of the structure. The calculation of the output variable LPF – under a given single set of input parameters – takes about 32 h on a high performance computer. In addition to the extremely high computational cost, the LPF may depend in a non-differentiable manner on some of the input parameters, especially variations in the geometry. A classical sensitivity analysis of the complete structure is currently out of reach.

Engineering information on the variability of the input parameters usually consists of a central value and a coefficient or range of variation. The basic strategy for arriving at a sensitivity assessment will be to successively pinch the input parameters (that is, freeze them at their central value) and study the effect on the variability of the output. Among the numerous alternative views on sensitivity analysis (cf. e.g. [14]), we shall also pursue simulation methods that yield interval bounds on the output as well as variance-based methods.

We wish to do our analysis without artificial parametric assumptions and with as few calls of the finite element program as possible. We will explore the usability of the following four methods, modelling the input variability by means of

- random sets and Tchebycheff's inequality;
- fuzzy sets and Hartley-like measures;
- intervals and sampling from a Cauchy distribution;
- standard Monte Carlo simulation and resampling.

Sensitivity analysis with the aid of Monte Carlo methods will include the computation of partial rank correlation coefficients and Sobol indices. The first three methods belong to imprecise probability in its proper sense; the last method is of a standard probabilistic type and included for comparison. Imprecise probability versions of the latter variance-based methods have been proposed by [10], but were not pursued in this study due to the expected additional computational costs.

A detailed description of the respective methods will follow in five sections, with a final section devoted to a comparison of the methods. The question of modelling correlations between the input variables will be addressed in the appropriate sections.

The ARIANE 5 frontskirt is the part of the launcher that connects the tanks section with the payload section and also has to support the booster loads. It consists of a light weight shell structure reinforced by struts. The full finite element model is composed of shell elements and solid elements, altogether with two million degrees of freedom. The load proportionality factor is computed by means of a path following procedure that follows bifurcations as long as possible until failure of the structure is reached, indicated by numerical breakdown of the program at a point at which the determinant of the local stiffness matrix does not change sign.

In order to make a test of the sensitivity analysis methods feasible, we made two simplifications. First, a simplified finite element model keeping the global structure (Fig. 1) with about ninety thousand degrees of freedom was used, and second, no distinction of bifurcation or material failure was made, so that the terminal value of the LPF was taken as that value at which the finite element program failed to converge. No further investigation of the reason for non-convergence was undertaken. The computational cost for the simplified model was one hour per call of the program.

In the sensitivity analysis, up to 17 input parameters were taken into account. A terse description of the meaning of the parameters as well as their nominal values can be read off from Table 1. This was all information we had available; in particular, no information on possible correlations of the input variables was given to us – actually on purpose; the project was in part a blind-folded test to check whether the sensitivity study would reveal dependencies which were expected from an engineering viewpoint (and it successfully did). The coefficients of variation of the input variables were estimated – after discussions with various engineering experts and consulting the literature [32] – at 15%.

At this point, it appears important to note that we did *not* intend to develop an imprecise probability model of the launcher. Rather, imprecise probability methods are introduced here for computing and visualizing sensitivities. So, while an imprecise probability model might well end up having different coefficients of variation for the various input parameters, it would be counter-productive to enter into a sensitivity study with different coefficients of variation, as this definitely would introduce distorting information (see also [28]).

To aid the reader in assessing the sensitivity results, we mention what we computed as the total variability of the output variable LPF: A direct Monte Carlo simulation of size $n = 100$ with input variables uniformly distributed on an interval around μ_i of spread $\pm 0.15\mu_i$ produced an output range of [3.45, 3.65] for the LPF.

For background material on sensitivity analysis we refer to the Special Issue [13], in particular the survey article [14] as well as [6,7,12]; for random sets, to [24,26]; for random and fuzzy sets, to [9,19]; for probability boxes, to [5]; for a review on

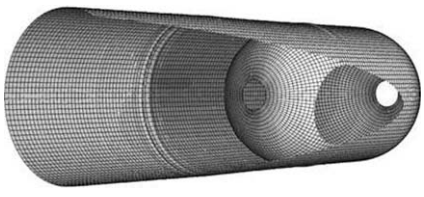

Fig. 1. Simplified finite element model of frontskirt.

Table 1
Description of input parameters no. 1–17.

i	Parameter X_i	Mean μ_i
1	Initial temperature	293 K
2	Step1 thermal loading cylinder1	450 K
3	Step1 thermal loading cylinder2	350 K
4	Step1 thermal loading cylinder3	150 K
5	Step1 thermal loading sphere1	150 K
6	Step1 thermal loading sphere2	110 K
7	Step2 hydrostatic pressure cylinder3	0.4 MPa
8	Step2 hydrostatic pressure sphere1	0.4 MPa
9	Step2 hydrostatic pressure sphere2	0.4 MPa
10	Step3 aerodynamic pressure	−0.05 MPa
11	Step4 booster loads y-direction node1	40,000 N
12	Step4 booster loads y-direction node2	20,000 N
13	Step4 booster loads z-direction node1	3.e6 N
14	Step4 booster loads z-direction node2	1.e6 N
15	Step4 mechanical loads x-direction	100 N
16	Step4 mechanical loads y-direction	50 N
17	Step4 mechanical loads z-direction	300 N

probabilistic treatment of uncertainty in structural engineering as well as information on variability of typical input parameters, to [32]. A survey of related ideas in risk analysis can be found in the tutorial [4] of the ISIPTA'07-conference and on concepts of generalized information theory in the tutorial [18].

2. Random set methods

It has been argued in [27,28] that random intervals constructed by Tchebycheff's inequality can serve as a non-parametric model of the variability of a parameter, given its mean value and variance as sole information. We begin with the univariate case of a real-valued random variable X. Let $\mu = E(X)$ be its expectation and $\sigma^2 = V(X)$ be its variance. Tchebycheff's inequality asserts that

$$P(|X-\mu| > d_\alpha) \leqslant \alpha, \quad d_\alpha = \sigma/\sqrt{\alpha}. \tag{1}$$

Equipping the unit interval $(0,1]$ with the uniform probability distribution, the non-parametric confidence intervals

$$I_\alpha = [\mu - d_\alpha, \mu + d_\alpha], \quad \alpha \in (0,1] \tag{2}$$

define a random set. By construction, the following formulas for the belief in the set I_α and the plausibility of its complement I_α^c hold:

$$\underline{P}(I_\alpha) = \int_{\{\beta\in(0,1]:I_\beta\subset I_\alpha\}} \mathrm{d}\beta = 1-\alpha \leqslant P(I_\alpha),$$
$$\overline{P}(I_\alpha^c) = \int_{\{\beta\in(0,1]:I_\beta\cap I_\alpha^c\neq\emptyset\}} \mathrm{d}\beta = \alpha \geqslant P(I_\alpha^c).$$

This shows that the random set description provides a conservative assessment of the variability of X. In applications, the range of the parameter X may be confined to a compact interval $[x_{\min}, x_{\max}]$. In this case, the random set will be truncated to

$$I_\alpha = [(\mu - d_\alpha) \vee x_{\min}, (\mu + d_\alpha) \wedge x_{\max}].$$

In the multivariate case $X = (X_1, \ldots, X_d)$ where each parameter X_i is modelled as a random set as in (2), we form the joint random set (assuming random set independence)

$$\alpha = (\alpha_1, \ldots, \alpha_d) \to A_\alpha = I^1_{\alpha_1} \times \cdots \times I^d_{\alpha_d}$$

again with the uniform distribution on the probability space $(0,1]^d$; see e.g. [1,2].

Let $g : \mathbb{R}^d \to \mathbb{R}$ be a continuous function, which will play the role of the input–output map in the sequel. If the input variables $X = (X_1, \ldots, X_d)$ are modelled as a random set A_α, $\alpha \in (0,1]^d$ (equipped with the uniform probability distribution), the output variable is given by the random set $g(A_\alpha)$, $\alpha \in (0,1]^d$. A coarse, but useful visualization of the output can be obtained by means of the upper and lower distribution functions (or *probability box*, [5])

$$\begin{aligned} \overline{F}(x) &= P(\alpha : g(A_\alpha) \cap (-\infty, x] \neq \emptyset) \\ \underline{F}(x) &= P(\alpha : g(A_\alpha) \subset (-\infty, x]). \end{aligned} \tag{3}$$

Another visualization of the output random set is by means of the *contour function* or *coverage function* [24]

$$C(x) = P(\alpha : x \in g(A_\alpha)).$$

Note that $\overline{F}(x)$ and $C(x)$ coincide as long as $\overline{F}(x) < 1$. The contour function is the membership function of the fuzzy set associated with the output random set [9].

In the numerical evaluation, the joint random set is approximated by a finite random set with focal elements

$$I^1_{\alpha_1} \times \cdots \times I^d_{\alpha_d}, \quad \alpha_j \in \left\{\frac{1}{n}, \frac{2}{n}, \ldots, 1\right\} \quad \text{for} \quad j = 1, \ldots, d,$$

each with probability weight n^{-d}. The input–output function is evaluated as follows: First, an interval $Q \subset \mathbb{R}^d$ is determined that bounds the relevant range of the input variables X. Next, the values of the function g are computed at the m^d nodes of a uniform grid on Q. The output $g(Q)$ is approximated by a response surface $\hat{g}(Q)$ obtained by multilinear splines. More precisely, to compute the image of one of the sets A_α, $\hat{g}(Q)$ is evaluated at all grid points inside A_α, at all points on its edges intersecting one of the grid lines, and at its vertices. The interval $g(A_\alpha)$ is approximated by the minimum and maximum value thus obtained. Finally, the probability box (3) is calculated by adding the weights when appropriate. The essential computational effort thus amounts to m^d calls of the finite element program.

The thin outer curves in Fig. 2 show the result of the calculation of the load proportionality factor (LPF) where the three input parameters X_3, X_{13}, X_{14} (temperature cylinder 2, booster load node 1 in z-direction, booster load node 2 in z-direction) were taken up as variable in the analysis (probability box on the left, contour function on the right). The variance σ^2 for the Tchebycheff model was adjusted such that the base intervals $[x_{\min}, x_{\max}]$ for each of the parameters was symmetric around the corresponding mean μ with spread $\pm 0.15\mu$. In this case, $d = 3$ and we chose $m = 5$ so that 125 calls to the FE-program were required.

We note that the one-dimensional random sets constructed from Tchebycheff's inequality are nested, but the higher dimensional ones generally are not. Thus special numerical methods that have been developed for consonant random sets (see e.g. [29]) are not applicable. In particular, the output random set does not consist of nested focal elements. Thus some information is lost when representing the output as a probability box or by its contour function. Nevertheless, this presentation appears useful for the purpose of visualizing the sensitivity.

Example 1. To assess the sensitivity of the load proportionality factor LPF with respect to the parameters X_3, X_{13}, X_{14} we use the Tchebycheff model for each of the parameters with spread 0.15 times their mean values. Then we successively set one of the resulting standard deviations $\sigma_3, \sigma_{13}, \sigma_{14}$ equal to zero (while keeping the others at their given value), go through the calculation indicated above and plot the resulting probability boxes and contour functions (solid lines – the thin lines indicate the unperturbed result). This is displayed in Fig. 2 and shows that setting $\sigma_{13} = 0$ produces the biggest reduction of the width of the probability box, while setting $\sigma_{14} = 0$ has little effect. We infer that the parameter X_{14} has the least influence on the variability of the response, while X_{13} exerts the biggest influence. For a way of quantifying this effect, see Section 3 and Table 2. The pinching strategy in the case of probability boxes is further explicated in [6] and applied in [28].

The question of dependence or interactivity of the input variables is a further issue. We note that no prior information on possible dependencies of the input variables was available in the project under study. We experimented with artificially introduced dependencies in order to evaluate their effect on the sensitivity of the output. Dependence could be modelled by copulas on the underlying probability space $(0,1]^d$ or by restrictions on the set of probability measures on $\mathbb{R}^d$ defined by the random set. Actually, we ran a number of tests with non-uniform joint distributions on $(0,1]^d$, given by copulas-including the smallest and largest copulas yielding the Fréchet–Hoeffding-bounds [25]. However, introducing dependence in this way turned out to have negligible effect on the output random set. Notions of (in)dependence based on restrictions on the set of probability measures include epistemic independence, strong independence and unknown interaction, cf. [8].

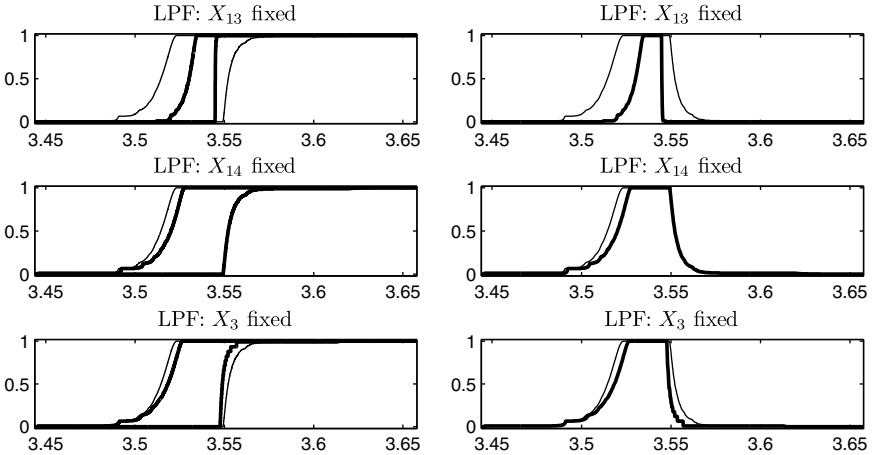

Fig. 2. LPF, total variability (thin lines) and LPF, successively pinched variables (solid lines); probability boxes (left) and contour functions (right).

Table 2
Hartley-like measures of fuzzy outputs, non-interactive vs. interactive input (left); Hartley-like measures of random set output (right).

Fuzzy set	HL-measure non-interactive	HL-measure interactive
No fixing	0.1481	0.1359
X_{13} fixed	0.0398	0.0315
X_{14} fixed	0.1430	0.0666
X_3 fixed	0.1268	0.1020
Random set		**HL-measure of p-box**
No fixing		0.0603
X_{13} fixed		0.0233
X_{14} fixed		0.0534
X_3 fixed		0.0504

The latter case is known to be computationally highly expensive. Thus we decided to remain with random set independence for our experiments and deferred a more detailed study of interactivity to the realm of fuzzy sets. A practicable approach for modelling interactivity will be presented in the following section on fuzzy sets.

3. Fuzzy sets

In this section, one-dimensional input variables will be modelled as *normalized fuzzy numbers*, that is as fuzzy subsets B of the real line with upper semi-continuous membership function $\pi_B(x)$ that attains the value 1. The α-level set of B is the set

$$B_\alpha = \{x \in \mathbb{R} : \pi_B(x) \geqslant \alpha\}, \quad \alpha \in (0,1].$$

In the multivariate case, the non-interactive joint fuzzy set is defined as follows. Given d univariate fuzzy sets $B^1, \ldots, B^d$, the joint fuzzy set has the α-level sets

$$B_\alpha = B^1_\alpha \times \cdots \times B^d_\alpha, \quad \alpha \in (0,1].$$

Interactivity will be modelled by certain parametric restrictions on the α-level sets. To avoid combinatorial complications, we shall treat interactivity of at most two out of the d variables. Since an α-level set of the form $B^i_\alpha \times B^j_\alpha$ is a homothetic image of the unit square, it suffices to give the definitions for $B^1_\alpha = B^2_\alpha = [0,1]$. Following [36], interactivity will be modelled by replacing the unit square by a diamond-shaped region, symmetric around one of the diagonals. Let $0 \leqslant \rho \leqslant 1$ and define the points $P_1, \ldots, P_4$ by

$$P_1 = (\rho/2, \rho/2), \qquad P_2 = (1-\rho/2, \rho/2),$$
$$P_3 = (1-\rho/2, 1-\rho/2), \quad P_4 = (\rho/2, 1-\rho/2).$$

Interactivity of *positive degree* ρ is modelled by taking the rhombus with vertices $(0,0)$, P_2, $(1,1)$, P_4 as joint level set, while interactivity of *negative degree* $-\rho$ is modelled by the rhombus with vertices $(0,1)$, P_1, $(1,0)$, P_3 as joint level set (Fig. 3). Let $g : \mathbb{R}^d \to \mathbb{R}$ be a continuous function. If the input variables $X = (X_1, \ldots, X_d)$ are modelled as a non-interactive or interactive fuzzy set with α-level sets B_α as above, Zadeh's extension principle yields the output variable as the fuzzy number with level sets $g(B_\alpha)$, $\alpha \in (0,1]$.

While a fuzzy set can be interpreted as a random set (cf. e.g. [9]) and the procedure appears similar to the one of Section 2, there is a fundamental difference in the multivariate case: in fuzzy set theory, only α-level sets of the same level are combined to produce the joint fuzzy set, while for random sets, the focal elements are obtained as products with respect to any combination and thus are indexed by the product space $(0,1]^d$.

Example 2. In the assessment of the sensitivity of the load proportionality factor LPF with respect to the input parameters X_3, X_{13}, X_{14}, these parameters were modelled as symmetric triangular fuzzy numbers,[4] with central values μ_i from Table 1 and spread $\pm 0.15\mu_i$ as before. The numerical calculation is based on the response surface method explained in Example 1. The images of the α-level sets are again computed by piecewise multilinear combination. To handle possible lack of monotonicity of the function g, we start with level $\alpha = 1$ and go the way down to $\alpha = 0$, insuring at each step that the approximations satisfy $g(A_\beta) \subset g(A_\alpha)$ for $\alpha < \beta$.

In the non-interactive case, the procedure for determining the sensitivity of the output with respect to the input variables is the same as in Example 1. The initial calculation is performed with proportional spreads $\pm 0.15\mu_i$. Then we successively replace one of the triangular fuzzy numbers by its crisp central value μ_i, and compute the output as a fuzzy number. The result gives a good visual representation of the change of variability. This can be quantified using e.g. the Hartley-like measure

[4] Triangular fuzzy numbers were employed for two reasons: first, they do not encode information other than a central value and a spread; second, they appear to be ideally suited for sensitivity analysis. In fact, they are built up linearly from nested intervals – this allows to read off the sensitivity of the output level by level and gives information on how the sensitivity changes when the input intervals increase.

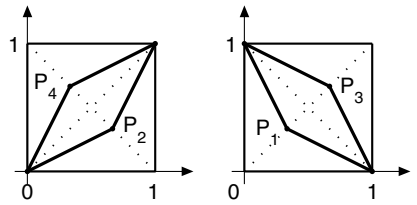

Fig. 3. Positive/negative interactivity.

$$\mathrm{HL}(B) = \int_0^1 \log_2(1 + \lambda(B_\alpha))\mathrm{d}\alpha$$

of fuzzy sets B as proposed by [19], where λ denotes Lebesgue measure (see also [2] for further implementation of this idea with random sets and [10] for interval-valued indices). The result is depicted in Fig. 4 (left), where the outer contour is the membership function of the fuzzy LPF with all input parameters fuzzy, while the shaded region is bounded by the membership function of the fuzzy LPF with successively pinched input parameters. It confirms the observations obtained by the random set method: X_{13} is the most influential parameter, followed by X_3 and then X_{14}. This can be explained by the model set-up: X_{13} refers to a large booster load on one side of the frontskirt, while X_{14} signifies a much smaller booster load on the opposite side. The Hartley-like measures displayed in Table 2 (left hand side, central column), though, show that some, albeit small, influence of parameter X_{14} is detectable. For reasons of comparison we also display the Hartley-like measure of the random set output in Table 2 (right hand side). The latter Hartley-like measures were computed from the level sets of the probability box as in Fig. 2.

Example 3. This example serves to show how the effect of possible correlations between two of the input parameters on the sensitivity can be assessed. *Correlation* will be interpreted here as degree of interactivity as described above. In this example, we assume a degree of interactivity $\rho = 0.8$ between parameters X_{13} and X_{14}. The remaining parameters are treated as non-interactive. The α-level sets are of cylindrical shape with a rhombic base R_α, say. Their images are again computed by piecewise multilinear combination. Otherwise, the procedure of successively pinching variables is similar: for example, when X_{13} is frozen at its central value μ_{13}, the interactivity restricts X_{14} to vary along the intersection of R_α with the line through μ_{13} parallel to the x_{14}-axis, while X_3 varies in its original α-level interval.

The result is shown in Fig. 4 (right). The outcome confirms the prominence of parameter X_{13}; as a consequence of the correlation, parameter X_{14} is seen to exert a comparable influence. The result also demonstrates that the correlation changes the sensitivity of the output with respect to parameter X_3. Table 2 (left hand side, right column) again shows the Hartley-like measures of the fuzzy output under successive pinching of input variables. One may note that the study of the influence of correlations can be implemented in the fuzzy approach with ease.

As in Example 1, the computational effort using the response surface consisted in 125 calls of the finite element program. The vertical jumps of the membership function in Fig. 4 (right) indicate that the output does not depend monotonically on the input variables. Closer inspection (done by producing an array of two-dimensional plots of the partial maps $X_i \to \mathrm{LPF}$) showed that this is indeed the case. Therefore, the accuracy of the method using just 125 grid values is in question. A number of additional explicit evaluations showed that the accuracy of the boundaries of the α-level sets for the LPF is in the range of

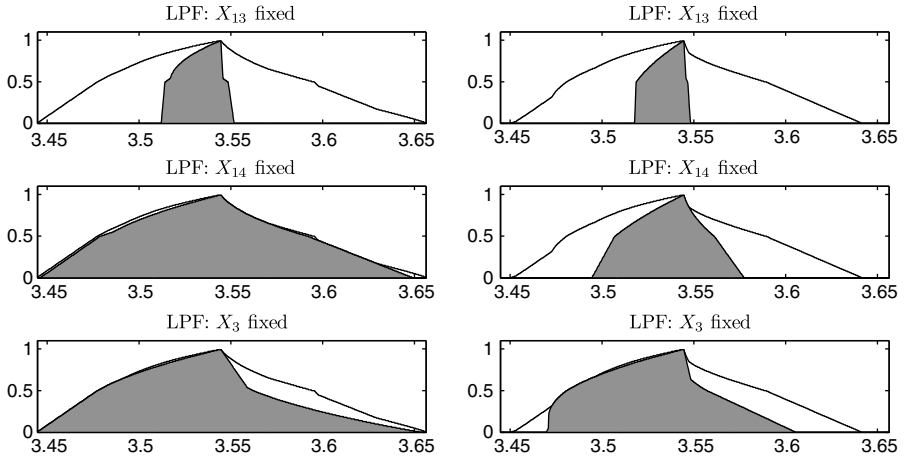

Fig. 4. Fuzzy sets: LPF, pinched variables, non-interactive case (left) and interactive case (right).

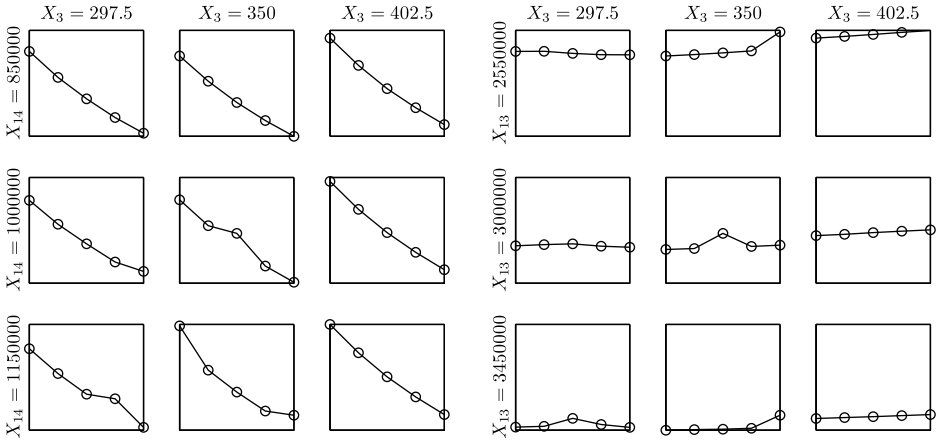

Fig. 5. Plots of partial maps X_{13} (abscissa), respectively X_{14} (abscissa), vs. LPF (ordinate) in the relevant range.

± 0.02 in absolute value. Fig. 5 shows that the partial map $X_{14} \to \text{LPF}$ is not monotonic, while the partial map $X_{13} \to \text{LPF}$ is monotonic within the considered range.

4. Interval bounds

This section is devoted to the most elementary imprecise probability model: interval estimates of input and output parameters, supposing that the variability of each input parameter X_i is described by an interval $[\mu_i - \Delta_i, \mu_i + \Delta_i]$ of spread Δ_i around a central value μ_i. Following the suggestion of [21], we use Monte Carlo simulation with the Cauchy distribution to compute an estimate of the output interval.

The underlying theory from [21] is as follows. Suppose we wish to estimate the difference

$$\Delta y = g(x_1, \ldots, x_d) - g(\mu_1, \ldots, \mu_d),$$

where $|\Delta x_i| = |x_i - \mu_i| \leqslant \Delta_i$. Linearization around the mean value gives

$$|\Delta y| \leqslant \Delta = \sum_{i=1}^{d} |c_i| \Delta_i, \quad c_i = \frac{\partial g}{\partial x_i}(\mu_1, \ldots, \mu_d).$$

If the X_i are independent random variables following a Cauchy distribution with scale parameter Δ_i, then $Y = c_1 X_1 + \cdots + c_d X_d$ obeys a Cauchy distribution with scale parameter $\Delta = |c_1|\Delta_1 + \cdots + |c_d|\Delta_d$. This offers the possibility of computing the bound Δ on the output spread by Monte Carlo simulation.

The algorithm runs along the following lines. To produce a single realization, a d-dimensional sample $(z_1, \ldots, z_d)$ of Cauchy distributed variables with scale parameters 1 is taken. Setting $K = \max_{1 \leqslant i \leqslant d} |z_i|$, one has that $\delta_i = \Delta_i z_i / K$ has a Cauchy distribution with scale parameter Δ_i / K. Putting $x_i = \mu_i + \delta_i$ it follows that:

$$Z = K(g(x_1, \ldots, x_d) - g(\mu_1, \ldots, \mu_d))$$

is a realization of a Cauchy distributed variable with desired scale parameter Δ (this is true exactly when g is linear and otherwise approximately). An n-fold repetition yields the Monte Carlo sample of size n of the variable Z. Fitting a Cauchy distribution – e.g. by the maximum likelihood method – produces an estimate of the spread Δ of the output interval $[g(\mu_1, \ldots, \mu_d) - \Delta,\ g(\mu_1, \ldots, \mu_d) + \Delta]$. The computational effort for this estimate is n calls of the finite element program and thus independent of the dimension d. This offers the possibility to include a larger number of input variables in the analysis.

The reason for using the Cauchy distribution is twofold. First, its parameter Δ is a direct estimate of the sought after spread of the output. Second, as has been argued in [21,22], it is necessary to use an unbounded distribution if one wants to get numerically accurate simulation results for the spreads of interval data. In fact, it is shown in [22] that the Cauchy distribution is the only distribution whose parameters transform according to the formula $\Delta = |c_1|\Delta_1 + \cdots + |c_d|\Delta_d$ under linear combinations.

Example 4. In this calculation, 17 input parameters were included with nominal values displayed in Table 1. The spreads Δ_i were taken as 0.15-times the nominal values μ_i. We used a direct Monte Carlo method to produce a sample of size $n = 100$. The value of the load proportionality factor LPF was obtained as $\mu = g(\mu_1, \ldots, \mu_d) = 3.5443$. The simulation resulted in an estimate for its spread of $\widehat{\Delta} = 0.2924$.

In the next step, the distribution of the resulting spread Δ was estimated by resampling. We employed 10,000 random subsamples of size 100 (with repetition), following the suggestions in [31]. This resulted in a 95%-confidence interval for Δ of $CI_{0.95}(\widehat{\Delta}) = [0.2281, 0.3685]$. The essential computational effort consisted in $n = 100$ calls of the finite element program.

Remark 5. A sensitivity analysis could be based on this method, again by pinching variables successively. It is possible to reduce computational cost by using the same Monte Carlo sample and approximating the pinched variables by a truncated Cauchy distribution. More precisely, instead of setting $\Delta_1 = 0$, say, we select the random numbers $(x_2, \ldots, x_d)$ computed above from the part of the population $(x_1, x_2, \ldots, x_d)$ which satisfies $|\delta_1| < \varepsilon$ for a suitably chosen small ε. This is justified, because the resulting truncated $(d-1)$-dimensional random variables converge in distribution to the ones with Δ_1 frozen at the value 0 as $\varepsilon \to 0$. However, successive simultaneous pinching of two or more variables requires repeated Monte Carlo simulation because the sample size would be too small for repeated truncation.

A more troublesome observation concerns the accuracy of the Cauchy method in our situation where the output function g is a nonlinear finite element computation resulting in the LPF. It turned out that the simulations of the auxiliary variable Z actually failed the Kolmogorov–Smirnov-test for being Cauchy distributed. This means that our output function g was too far away from linearity and thus puts the accuracy of the Cauchy method into question in this context.

5. Monte Carlo simulation

To complete the analysis, we shall discuss the merits of direct Monte Carlo simulation in sensitivity analysis. For the sake of comparison, we place ourselves in the standard probabilistic setting. As noted earlier, the purpose of this paper is not to implement an imprecise probability model of the system under consideration, but rather study the sensitivity of the output with respect to variations of the input parameters. Thus the variability of the input is introduced here for *computational purposes*. For this, standard, probabilistic Monte Carlo simulation is a viable option, and contrasts the imprecise probability techniques discussed in the previous sections.

To be sure, it is possible to construct imprecise versions of the sensitivity indices we use, and even employ Monte Carlo techniques to compute them. This is needed when starting from an imprecise probability model of the structure and has been proposed in [10]. In view of the expected increase in computational cost and the general purpose of the paper we did not work out this branch of analysis.

In the Monte Carlo simulation to follow, we will use uniformly distributed input variables. This choice is motivated by the purpose of our study: modelling the variability of the input with the smallest amount of information necessary so as not to introduce information that might distort the simulated sensitivities. Symmetric triangular distributions offer another option; for the sake of exposition, we remain with uniformly distributed input here.

An explorative analysis usually starts with checking the scatterplots of individual input variables vs. the output, obtained by Monte Carlo simulation. Another common method is to compute the weighted contribution of each input variable to the variance of the output. These methods suffer from the problem that hidden interactions may have a significant effect on the decomposition of the variance (see, however, [3]). We therefore turn to a method which intends to remove the influence of co-variates on the correlation between a given input variable X_i and the output variable Y. This method is based on the partial correlation coefficient (PCC) or the partial rank correlation coefficient (PRCC). For reasons of comparison, we shall also compute various other indicators for interactivity or correlation.

We recall that partial correlation between two random variables X_i and Y given a set of co-variates $X_{\setminus i} = \{X_1, \ldots, X_{i-1}, X_{i+1}, \ldots, X_d\}$ is defined as the correlation between the two residuals $e_{X_i \cdot X_{\setminus i}}$ and $e_{Y \cdot X_{\setminus i}}$ obtained by regressing X_i on $X_{\setminus i}$ and Y on $X_{\setminus i}$, respectively. More precisely, one first constructs the two regression models

$$\widehat{X}_i = \alpha_0 + \sum_{j \neq i} \alpha_j X_j, \quad \widehat{Y} = \beta_0 + \sum_{j \neq i} \beta_j X_j,$$

obtaining the residuals

$$e_{X_i \cdot X_{\setminus i}} = X_i - \widehat{X}_i, \quad e_{Y \cdot X_{\setminus i}} = Y - \widehat{Y}.$$

Since $e_{X_i \cdot X_{\setminus i}}$ and $e_{Y \cdot X_{\setminus i}}$ are those parts of X_i and Y that remain after subtraction of the best linear estimates in terms of $X_{\setminus i}$, the partial correlation coefficient

$$\rho_{X_i, Y \cdot X_{\setminus i}} = \rho(e_{X_i \cdot X_{\setminus i}}, e_{Y \cdot X_{\setminus i}})$$

quantifies the linear relationship between X_i and Y after removal of any part of the variation due to the linear influence of $X_{\setminus i}$. Applying a rank transformation to the variables X_i and Y leads to the partial rank correlation coefficient (PRCC). For further background on PCCs and PRCCs, see [11,15,30].

Example 6. To estimate the influence of each of the 17 input parameters from Table 1 on the output LPF, we performed a Monte Carlo simulation of size $n = 100$ with uniformly distributed input variables (on the intervals as in Example 4), using Latin hypercube sampling, an efficient stratified sampling strategy.

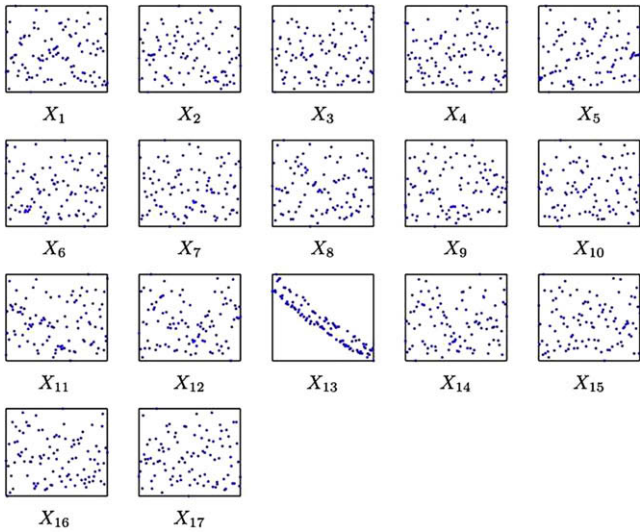

Fig. 6. Scatterplots of 17 input variables vs. output.

To obtain a sample of size n, the Latin hypercube sampling plan divides the range of each variable X_i into n disjoint subintervals of equal probability. First, n values of each variable X_i, $i = 1, \ldots, d$, belonging to the respective subintervals are randomly selected. Then the n values for X_1 are randomly paired without replacement with the n values for X_2. The resulting pairs are then randomly combined with the n values of X_3 and so on, until a set of n d-tuples is obtained. This set forms the Latin hypercube sample. The advantage of Latin hypercube sampling is that sampled points are evenly distributed through design space, thereby covering regions possibly important for the input–output map which might be missed by direct Monte Carlo simulation. It can be shown that the variance of an estimator based on Latin hypercube sampling is asymptotically smaller than the variance of the direct Monte Carlo estimator, and possibly markedly smaller when the input–output map is partially monotonic [12,23,35].

For additional accuracy in view of the rather small sample size we subjected the simulated variables to correlation control (see [16,17]). This procedure consists in a rearrangement of the originally simulated values such that the resulting empirical rank correlation matrix is close to diagonal.

The scatterplot of Fig. 6 gives a first impression of the influence of the input variables on the output. However, as noted above, the scatterplot alone delivers questionable information. Accordingly, we computed various correlation coefficients that discount certain possible interactions between the input variables.

The results are displayed in Table 3; the meaning of the various coefficients is as follows:

Table 3
Various measures of correlation input–output; superscripts indicate the respective ranks.

Parameter number	Raw data			Rank data		
	CC	PCC	SRC	RCC	PRCC	SRRC
1	−0.0553	**−0.2631**^{3}	**−0.0662**^{3}	−0.0566	**−0.2788**^{4}	**−0.0659**^{4}
2	−0.0781	−0.0888	−0.0217	−0.0913	−0.1420	−0.0326
3	0.0954	**0.4680**^{2}	**0.1285**^{2}	0.0629	**0.3957**^{2}	**0.0978**^{2}
4	0.0553	0.1038	0.0254	0.0574	0.1173	0.0268
5	0.0525	0.0612	0.0149	0.0653	0.1315	0.0301
6	0.0418	0.0210	0.0051	0.0521	0.0720	0.0164
7	−0.0043	−0.0223	−0.0054	0.0062	0.0237	0.0054
8	−0.0397	−0.1230	−0.0301	−0.0233	−0.0629	−0.0143
9	0.0479	0.1787	0.0442	0.0684	**0.2753**^{5}	**0.0652**^{5}
10	0.0216	0.1803	0.0446	0.0237	0.1942	0.0450
11	−0.0181	0.0893	0.0219	−0.0332	0.0340	0.0077
12	0.0019	0.0203	0.0049	0.0152	0.0644	0.0147
13	**−0.9534**^{1}	**−0.9690**^{1}	**−0.9574**^{1}	**−0.9593**^{1}	**−0.9728**^{1}	**−0.9602**^{1}
14	0.0407	**0.2596**^{4}	**0.0653**^{4}	0.0380	**0.2810**^{3}	**0.0665**^{3}
15	0.0403	0.0352	0.0086	0.0498	0.0667	0.0152
16	−0.0844	−0.0880	−0.0216	−0.0777	−0.0805	−0.0184
17	−0.0056	0.0744	0.0181	−0.0050	0.0791	0.0180

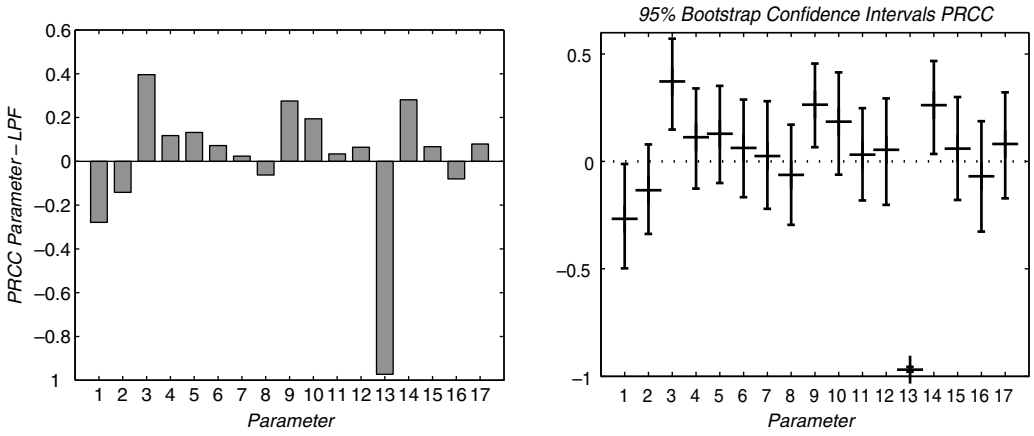

Fig. 7. Partial rank correlation coefficients (left) and confidence intervals (right).

- CC: Pearson correlation coefficient, quantifying the strength of a linear relationship between X_i and LPF;
- PCC: partial correlation coefficient, quantifying the strength of a linear relationship between X_i and LPF after removal of linear interactions with $X_{\setminus i}$;
- SRC: standardized regression coefficient between X_i and LPF, quantifying the effect of deviations from μ_i;
- RCC: Spearman rank correlation coefficient, quantifying the strength of a monotonic relationship between X_i and LPF;
- PRCC: partial rank correlation coefficient, quantifying the strength of a monotonic relationship between X_i and LPF after removal of monotonic interactions with $X_{\setminus i}$;
- SRRC: standardized rank regression coefficient between X_i and LPF, quantifying the effect of deviations from μ_i within a rank regression model.

The linear regression model constructed in order to obtain standardized regression coefficients (including all variables) has a corresponding R^2 of 0.9414, thus indicating a fairly good fit. Changing to rank transformed data only slightly improved the quality of approximation (yielding $R^2 = 0.9488$). The resulting sensitivity indices induce a ranking of the input parameters according to their influence on the output (denoted by superscripts in Table 3). It is seen that the evaluations based on RCCs, PRCCs and SRRCs do not differ drastically from those obtained from raw data (CCs, PCCs and SRCs).

The rankings of the input parameters were based on the absolute value of the index under study. Small index values may or may not be considered as significant. For this reason, we constructed bootstrap percentile confidence intervals with nominal level 0.95. In an overall assessment of the ranking, only those sensitivity estimates with a resultant confidence interval not including 0 (indicated by bold values) should be regarded as assertive.

As an example, we visualize the computed PRCCs in Fig. 7 (left). For further statistical confirmation, we performed a resampling procedure as in Example 4, producing bootstrap confidence intervals for the partial rank correlation coefficients as displayed in Fig. 7 (right). Accordingly, only the PRCCs of the parameters X_1, X_3, X_9, X_{13} and X_{14} test to be nonzero.

The outcome confirms the results of the sensitivity analysis in the previous sections: among the parameters X_3, X_{13} and X_{14}, the one with the biggest influence is X_{13}, followed by X_3 and X_{14}. In addition, it shows the influence of parameters that would not have been visible in the scatterplots of Fig. 6.

We also ran various tests with correlated input as in Example 3 which confirmed the observed sensitivities. However, each test required a new Monte Carlo simulation with sample size $n = 100$.

6. Sobol indices

A more sophisticated method for estimating the contribution of X_i to the total output variation are Sobol indices, based on the expansion of the input–output map g into summands of increasing dimensionality [33]. More precisely, assume the parameters X_i are independent and identically distributed according to a uniform distribution on the unit interval. Then the global output variance can be decomposed into

$$V\{g(X_1,\ldots,X_d)\} = \sum_{i=1}^{d} V\{g_i(X_i)\} + \sum_{i<j} V\{g_{ij}(X_i,X_j)\} + \cdots + V\{g_{1,2,\ldots,d}(X_1,\ldots,X_d)\}.$$

Consequently, the so-called *Sobol index*

$$S_{i_1,\ldots,i_s} = V\{g(X_1,\ldots,X_d)\}^{-1} V\{g_{i_1,\ldots,i_s}(X_{i_1},\ldots,X_{i_s})\}$$

quantifies the proportion of total variability due to the interplay between $(X_{i_1},\ldots,X_{i_s})$, $s \leqslant d$.

From a computational point of view, the terms of the sum above are defined via high dimensional integrals, e.g.

$$V\{g_i(X_i)\} = \int_{[0,1]} \left\{ \int_{[0,1]^{d-1}} g(x_1,\dots,x_d)\mathrm{d}x_1\cdots\mathrm{d}x_{i-1}\mathrm{d}x_{i+1}\cdots\mathrm{d}x_d - \int_{[0,1]^d} g(x_1,\dots,x_d)\mathrm{d}x_1\cdots\mathrm{d}x_d \right\}^2 \mathrm{d}x_i$$

and can be approximated by Monte Carlo integration schemes involving only function values of g, i.e. without having to explicitly construct $g_{i_1,\dots,i_s}$ (see also [34]).

As a mild generalization, the preceding partition is valid for subgroups of variables as well. Specifically, let $(X_1,\dots,X_d)$ be divided into two disjoint clusters of variables (Z_1,Z_2). Consequently,

$$V\{g(X_1,\dots,X_d)\} = V\{g(Z_1,Z_2)\} = V\{g_1(Z_1)\} + V\{g_2(Z_2)\} + V\{g_{1,2}(Z_2,Z_2)\}.$$

The corresponding Monte Carlo integration in this case reads

$$V\{g(X_1,\dots,X_d)\} \approx \frac{1}{n}\sum_{j=1}^{n} g(Z_1^{(j)},Z_2^{(j)})^2 - \left(\frac{1}{n}\sum_{j=1}^{n} g(Z_1^{(j)},Z_2^{(j)})\right)^2$$

and

$$V\{g_1(Z_1)\} \approx \frac{1}{n}\sum_{j=1}^{n} g(Z_1^{(j)},Z_2^{(j)})g(Z_1^{(j)},\widetilde{Z}_2^{(j)}) - \left(\frac{1}{n}\sum_{j=1}^{n} g(Z_1^{(j)},Z_2^{(j)})\right)^2,$$

where $Z_2^{(j)}$ and $\widetilde{Z}_2^{(j)}$ are independent. An analogous formula holds for $V\{g_2(Z_2)\}$. Thus the estimation of $V\{g_1(Z_1)\}$ and hence of the associated Sobol index requires $2n$ Monte Carlo trials: n in order to obtain

$$g(Z_1^{(j)},Z_2^{(j)}), \quad j = 1,\dots,n$$

and another n to compute

$$g(Z_1^{(j)},\widetilde{Z}_2^{(j)}), \quad j = 1,\dots,n.$$

Consequently, the simulated values of Z_1 are reused, while a new sampling matrix has to be generated for the variables in Z_2.

Example 7. Grouping the 17 input variables according to their rankings in Table 3, two sets were defined, namely

$$Z_1 := (X_1,X_3,X_{13})$$

representing the supposedly important parameters and

$$Z_2 := (X_2,X_4,\dots,X_{12},X_{14},\dots,X_{17})$$

containing less decisive input quantities. The primary aim was to support our previous sensitivity analysis results, i.e. to reconfirm the dominance of Z_1 on the LPF value.

Estimating the individual contributions to the variability of the LPF due to Z_1 and Z_2 required two auxiliary Monte Carlo simulation of size $n = 100$, conducted with the same underlying sampling matrix as in the computation of Table 3 but newly generated columns for the variables in Z_1 and Z_2, respectively. Care was exercised to maintain the integrity of the original Latin hypercube and rank correlation structure.

As remarked in [30] – and confirmed by our experiments – it is numerically more robust to compute the Sobol indices above on the ranks of the terms $g(Z_1^{(j)},Z_2^{(j)}),\dots$ rather than the terms themselves. This calculation yielded the indices

$$\widehat{S}_{\{1,3,13\}} = 0.966, \quad CI_{0.95}(\widehat{S}_{\{1,3,13\}}) = [0.944, 0.977]$$

and

$$\widehat{S}_{\{2,4,\dots,12,14,\dots,17\}} = 0.116, \quad CI_{0.95}(\widehat{S}_{\{2,4,\dots,12,14,\dots,17\}}) = [-0.084, 0.307].$$

Again the confidence intervals were determined by resampling, using 5000 subsamples. Due to small sample size, the numerical accuracy of the Monte Carlo estimators for the Sobol indices is unsatisfactory. Nevertheless, the conclusions drawn in the foregoing are consolidated: the larger part of the total LPF variability is being explained by the parameters in Z_1.

It should be emphasized that despite their universality Sobol indices have to carry the burden of computational inefficiency: determining all indices requires $2^d - 1$, calculating the main effects of all variables $2d + 1$ Monte Carlo studies of size n each. In the context of very time-consuming models the applicability of this approach hence is limited to the validation of inexpensive sensitivity analysis results as sketched above.

7. Summary and conclusions

Starting from a research project in aerospace engineering one of whose goals was to determine the sensitivity of the buckling load of the frontskirt of the ARIANE 5 launcher with respect to certain input parameters, we explored various methods

from probability and imprecise probability theory. In view of the excessive computational costs of a single run of the finite element program, the major challenge was to develop methods with as few calls of the program as possible. We used a simplified model of the launcher for the numerical tests of the methods.

The methods under scrutiny were random sets and Tchebycheff's inequality, fuzzy sets and Hartley-like measures, intervals and sampling from a Cauchy distribution, standard Monte Carlo simulation and resampling. Criteria for the evaluation are

- computational effort;
- applicability to large scale problems;
- accuracy;
- avoidance of tacit assumptions;
- reliability and clarity of interpretation;
- possibility of analyzing correlated input.

Generally speaking, the Monte Carlo simulation methods are computationally least expensive. For our sensitivity study, a sample size of $n = 100$ appeared sufficient. In addition – as is well known – the sample size can be chosen independently of the number of input variables, so that we could include all 17 variables in our study. These methods are clearly applicable to large scale problems. A disadvantage is that pinching of variables requires repetition of the $n = 100$ simulations. Thus computing PRCCs plus resampling is possible irrespective of the problem scale, but variance decomposition by pinching variables is not. The same applies to analyzing sensitivity with respect to input correlations, which requires repetition of the simulation as well. Sobol indices constitute a well-founded method of estimating the contribution of each input variable to the total output variation. However, the computational effort increases dramatically with the number of indices one wishes to calculate. Thus in the context of time-consuming computational models the applicability of this approach is limited to studying the influence of a small number of grouped variables.

The numerical accuracy of the Monte Carlo simulation is well known to be of order $1/\sqrt{n}$ times the standard deviation of the simulated variable. In view of the coefficients of variation which were in the range of 10% this appeared sufficient for the sensitivity study.

We emphasize that the results of a Monte Carlo simulation are amenable to resampling, which introduces little additional computational effort (no further evaluations of the costly input–output map are needed). In this way, bootstrap confidence intervals can be obtained that may serve as statistical estimates of the accuracy of the results. For example, we estimated the bias of each partial rank correlation coefficient, that is, the absolute value of the difference of the mean of the resampled data and the initial estimate. The estimated bias resulted to be less than 2% of the initial estimate. Further, the significance of the resulting ranking of the influence of the respective input parameters can be assessed by comparing the bootstrap confidence intervals.

The Cauchy method is a simulation method for estimating the spread of the output interval. The resulting estimate is non-parametric in as much as only the spreads of the input variables enter. As a subcase of Monte Carlo simulation, everything that has been said above applies here as well. A possibly problematic point is that the method is derived under the assumption that the output function is approximately linear. In our case, the output function is substantially nonlinear. The accuracy can be improved by the suggestion of [21] of repeated bisection of the input interval or by the quadratic approach proposed in [22], though at an increase in computational cost.

Both in the fuzzy set and random set methods, the output α-level sets and focal sets, respectively, are computed by searching for the maximum and minimum of the corresponding output range. Sufficient accuracy can only be obtained by a larger number of calls of the output function, evaluated on a grid of input data. In addition, the grid size increases exponentially with the number of input variables. These methods appear feasible only in the case of medium size problems and a small number of input variables. Monotonicity or partial monotonicity of the output function increases accuracy and helps reducing the number of computations required. We note that simulation methods for computing upper and lower probabilities have also been put forth in the literature, e.g. in [1,10]; but were not pursued in this study.

Test runs with additional point evaluations showed that the numerical error of the interpolation (i.e. replacing the true output function by a piecewise bilinear response surface) was less than 1%, thus definitely satisfactory. However, the optimization error introduced when calculating the boundaries of the output level sets turned out to be about ± 0.02 in absolute value, which is around 10–20% of the spread of the base level (see end of Section 3).

The numerical error in the boundaries of the output level sets appears less influential in the random set method. This is due to a certain averaging effect. Indeed, in the fuzzy model the computation of ℓ output level sets corresponds to ℓ input level sets, whereas in the random set model – at least when using random set independence – a combination of ℓ^d input focal sets enters (d the number of variables).

Both methods are essentially non-parametric. The random set model we used is generated by Tchebycheff's inequality and hence non-parametric by definition. In the fuzzy set model, we used triangular fuzzy numbers as input. These can be seen as a collection of intervals of linearly changing length. The α-level sets resulting from the computation determine the output range when the input varies over d-dimensional intervals of length proportional to $1 - \alpha$.

The fuzzy model in combination with the response surface technique has an additional advantage: it allows the a posteriori introduction of interactivity between the input variables without the need for new calls of the output function. The

effect of interactive input can simply be evaluated by interpolation in the response surface. Interactivity has been modelled by distorting the joint α-level sets – this led to a visible change in the sensitivities. In contrast – in the random set model – keeping the joint focal sets and introducing dependence of the input variables by means of copulas on the underlying probability space showed little effect on the sensitivity of the output.

We finally comment on the practicality of upscaling to the full problem. This remains a major challenge. The computational structure of the given problem consists in a nonlinear, incremental procedure. The LPF is obtained as the ultimate load value beyond which the computed solution cannot be prolonged. This may be either due to a bifurcation point or to a breakdown of the structure. As noted in the introduction, this was not distinguished in the simplified model; in the full model, a path following procedure is put in effect at bifurcation points so that the ultimate load value would correspond to material breakdown. In order to arrive at a sensitivity analysis of the full model, we plan to pursue two strategies. One strategy is a perturbation method that replaces the full model by a quadratic approximation when a bifurcation point is reached. This is based on Koiter's asymptotic analysis of post-buckling of shells, see e.g. [20]. The sensitivity analysis would be done with the asymptotic model in place of the full model. The second strategy is to start the sensitivity analysis at a later stage of the iterative procedure. Both methods require to access the finite element code at a deeper level. A certain difficulty which we expect to encounter stems from the fact that the incremental procedure is path dependent. Thus varying the input parameters late in the process could be misleading, as initial variations might result in a quite different path to breakdown.

Acknowledgements

We are grateful to Herbert Haller for providing the finite element models and advice on engineering questions. Thanks are also due to Christof Neuhauser and Alexander Ostermann for discussions on numerical problems, to Hermann Starmans for the project management and to Robert Winkler for help with the finite element codes.

References

[1] D.A. Alvarez, On the calculation of the bounds of probability of events using infinite random sets, International Journal of Approximate Reasoning 43 (2006) 241–267.
[2] D.A. Alvarez, Nonspecificity for infinite random sets of indexable type, Fuzzy Sets and Systems 159 (2008) 289–306.
[3] G.E.B. Archer, A. Saltelli, I.M. Sobol, Sensitivity measures, ANOVA-like techniques and the use of the bootstrap, Journal of Statistical Computation and Simulation 58 (1997) 99–120.
[4] S. Ferson, Risk analysis: rough but ready tools for calculations under variability and uncertainty, in: Tutorial, ISIPTA'07 – Fifth International Symposium on Imprecise Probability: Theories and Applications, Prague, 2007. <http://www.sipta.org/isipta07/tutorials.html>.
[5] S. Ferson, V. Kreinovich, L. Ginzburg, D.S. Myers, K. Sentz, Constructing probability boxes and Dempster–Shafer structures, SANDIA Report SAND2002-4015, Sandia National Laboratories, Albuquerque, 2003.
[6] S. Ferson, W.T. Tucker, Sensitivity analysis using probability bounding, Reliability Engineering and System Safety 91 (2006) 1435–1442.
[7] S. Ferson, W.T. Tucker, Sensitivity in risk analysis with uncertain numbers, SANDIA Report SAND2006-2801, Sandia National Laboratories, Albuquerque, 2006.
[8] Th. Fetz, M. Oberguggenberger, Propagation of uncertainty through multivariate functions in the framework of sets of probability measures, Reliability Engineering and Systems Safety 85 (2004) 73–87.
[9] I.R. Goodman, H.T. Nguyen, Fuzziness and randomness, in: C. Bertoluzza, M.Á. Gil, D.A. Ralescu (Eds.), Statistical Modeling Analysis and Management of Fuzzy Data, Physica-Verlag, Heidelberg, 2002.
[10] J.W. Hall, Uncertainty-based sensitivity indices for imprecise probability distributions, Reliability Engineering and System Safety 91 (2006) 1443–1451.
[11] J.C. Helton, F.J. Davis, Sampling-based methods for uncertainty and sensitivity analysis, SANDIA Report SAND99-2240, Sandia National Laboratories, Albuquerque, 2000.
[12] J.C. Helton, F.J. Davis, Latin hypercube sampling and the propagation of uncertainty in analyses of complex systems, SANDIA Report SAND2001-0417, Sandia National Laboratories, Albuquerque, 2002.
[13] J.C. Helton, R.M. Cooke, M.D. McKay, A. Saltelli (Eds.), The Fourth International Conference on Sensitivity Analysis of Model Output (SAMO 2004), Santa Fe, New Mexico. Special Issue, Reliability Engineering and System Safety 91(10–11) (2006) 1105–1474.
[14] J.C. Helton, J.D. Johnson, C.J. Sallaberry, C.B. Storlie, Survey of sampling-based methods for uncertainty and sensitivity analysis, Reliability Engineering and System Safety 91 (2006) 1175–1209.
[15] R.L. Iman, W.J. Conover, The use of the rank transformation in regression, Technometrics 21 (1979) 499–509.
[16] R.L. Iman, W.J. Conover, A distribution-free approach to inducing rank correlation among input variables, Communications in Statistics – Simulation and Computation 11 (1982) 311–334.
[17] R.L. Iman, M.J. Shortencarier, J.D. Johnson, A FORTRAN 77 program and user's guide for the calculation of partial correlation and standardized regression coefficients, SANDIA Report SAND85-0044, Sandia National Laboratories, Albuquerque, 1985.
[18] G. Klir, Generalized information theory, in: Tutorial, ISIPTA'07 – Fifth International Symposium on Imprecise Probability: Theories and Applications, Prague, 2007. <http://www.sipta.org/isipta07/tutorials.html>.
[19] G. Klir, M.J. Wiermann, Uncertainty-Based Information Elements of Generalized Information Theory, Physica-Verlag, Heidelberg, 1998.
[20] W.T. Koiter, Current trends in the theory of buckling, in: B. Budiansky (Ed.), Buckling of Structures. Proceedings IUTAM Symposium, Cambridge 1974, Springer-Verlag, Berlin, 1976.
[21] V. Kreinovich, S.A. Ferson, A new Cauchy-based black-box technique for uncertainty in risk analysis, Reliability Engineering and and System Safety 85 (2004) 267–279.
[22] V. Kreinovich, J. Beck, C. Ferregut, A. Sanchez, G.R. Keller, M. Averill, S.A. Starks, Monte-Carlo-type techniques for processing interval uncertainty, and their potential engineering applications, Reliable Computing 13 (2007) 25–69.
[23] M.D. McKay, R.J. Beckman, W.J. Conover, A comparison of three methods for selecting values of input variables in the analysis of output from a computer code, Technometrics 21 (1979) 239–245.
[24] I. Molchanov, Theory of Random Sets, Springer-Verlag, Berlin, 2005.
[25] R.B. Nelsen, An Introduction to Copulas, second ed., Springer Science + Business Media Inc., New York, 2006.
[26] H.T. Nguyen, An Introduction to Random Sets, Chapman & Hall, Boca Raton, 2006.

[27] M. Oberguggenberger, W. Fellin, Assessing the sensitivity of failure probabilities: a random set approach, in: G. Augusti, G.I. Schuëller, M. Ciampoli (Eds.), Safety and Reliability of Engineering Systems and Structures, ICOSSAR 2005, Rome, Millpress, Rotterdam 2005, pp. 1755–1760.
[28] M. Oberguggenberger, W. Fellin, Reliability bounds through random sets: nonparametric methods and geotechnical applications, Computers and Structures 86 (2008) 1093–1101.
[29] M. Oberguggenberger, S. Pittschmann, Differential equations with fuzzy parameters, Mathematical and Computer Modelling of Dynamical Systems 5 (1999) 181–202.
[30] A. Saltelli, I.M. Sobol, About the use of rank transformation in sensitivity analysis of model output, Reliability Engineering and System Safety 50 (1995) 225–239.
[31] J. Shao, D.-S. Tu, The Jackknife and Bootstrap, Springer-Verlag, New York, 1995.
[32] G.I. Schuëller, On the treatment of uncertainties in structural mechanics and analysis, Computers and Structures 85 (2007) 235–243.
[33] I.M. Sobol, Sensitivity analysis for nonlinear mathematical models, Mathematical Modeling and Computational Experiment 1 (1993) 407–414.
[34] I.M. Sobol, Global sensitivity indices for nonlinear mathematical models and their Monte Carlo estimates, Mathematics and Computers in Simulation 55 (2001) 271–280.
[35] M. Stein, Large sample properties of simulations using Latin hypercube sampling, Technometrics 29 (1987) 143–151.
[36] F. Tonon, C.L. Pettit, Toward a definition and understanding of correlation for variables constrained by random relations, in: G. Augusti, G.I. Schuëller, M. Ciampoli (Eds.), Safety and Reliability of Engineering Systems and Structures, ICOSSAR 2005, Rome, Millpress, Rotterdam, 2005, pp. 1741–1745.